ResearchGate

See discussions, stats, and author profiles for this publication at: https://www.researchgate.net/publication/253779660

Design, development, and testing of a transonic missile fin employing PBP/DEAS actuators

Article *in* Proceedings of SPIE - The International Society for Optical Engineering · March 2008

DOI: 10.1117/12.774516

CITATIONS
4

READS
325

2 authors:

Ron Barrett
University of Kansas
119 PUBLICATIONS **1,178** CITATIONS
SEE PROFILE

Roelof Vos
Delft University of Technology
22 PUBLICATIONS **487** CITATIONS
SEE PROFILE

Some of the authors of this publication are also working on these related projects:

Thermadapt Theory View project

Post-buckled actuators View project

All content following this page was uploaded by Ron Barrett on 16 August 2014.

The user has requested enhancement of the downloaded file.

Design, Development and Testing of a Transonic Missile Fin Employing PBP/DEAS Actuators

Ron Barrett and Roelof Vos
Aerospace Engineering Department, The University of Kansas, Lawrence, Kansas USA

ABSTRACT

This paper describes a new class of flight control actuators using Post-Buckled Precompressed (PBP) piezoelectric elements mounted within a transonic missile fin. These actuators are designed to produce significantly higher deflection and force levels than conventional piezoelectric actuator elements. Classical laminate plate theory (CLPT) models are shown to work very well in capturing the behavior of the free, unloaded elements. A new high transverse deflection model which employs nonlinear structural relations is shown to successfully predict the performance of the PBP actuators as they are exposed to higher and higher levels of axial force, which induces post buckling deflections. A 6" (15.2cm) square rounded diamond transonic fin was made with integral PBP actuator elements. Quasi-static bench testing showed deflection levels in excess of ±7° at rates exceeding 21 Hz. The new solid state PBP actuator was shown to reduce the part count with respect to conventional servoactuators by an order of magnitude. Power consumption dropped from 24W to 1.3W, slop went from 1.6° to 0.02° and peak current draw went from 5A to 18mA. The PBP actuator was wind tunnel tested and shown to possess no flutter, divergence or adverse aeroelastic coupling characteristics.

Keywords: Piezoelectric Flight ControlPost-Buckled Precompressed Dynamic Elastic Axis Shifting

NOMENCLATURE

Symbol	Description	Units
a	integrating factor	
A, B, D	in-plane, coupled, bending laminate stiffnesses	lb/in, lb, in-lb (N/m, N, N-m)
AR	PBP Amplification Ratio = $\delta(F_a>0)/\ \delta(F_a=0)$	
b	actuator width	in (mm)
c	integrating factor	
E	stiffness	GPa (msi)
M	applied moment vector	N-m/m (in-lb/in)
N	applied force vector	N/m (lb/in)
t	thickness	in (mm)
y	out of plane displacement dimension	in (mm)
z	through thickness dimension	in (mm)
α	angle of attack	deg
δ	PBP beam angle	deg
δ_o	PBP end rotation angle	deg
ε	laminate in-plain strain	μstrain
κ	laminate curvature	rad/in (rad/m)
Λ	piezoelectric free element strain	μstrain
σ	stress	msi (GPa)
Subscripts		
a	actuator	
b	bond	
ex	external	
l	laminate	
s	substrate	
t	thermally induced	

Industrial and Commercial Applications of Smart Structures Technologies 2008,
edited by L. Porter Davis, Benjamin Kyle Henderson, M. Brett McMickell, Proc. of SPIE Vol. 6930,
693011, (2008) · 0277-786X/08/$18 · doi: 10.1117/12.774516

2008 SPIE Digital Library -- Subscriber Archive Copy

1. INTRODUCTION

The technical community has nearly a hundred years of modeling experience related to piezoelectric elements of many classes. From sonar to phonograph pickups to flaps on helicopter rotor blades, piezoelectric sheets and stacks have been used as driving elements.[1] Numerous studies have been centered on the addition of various types of mechanisms, the use of different lamination techniques and/or shapes to amplify either deflection at the expense of force or force at the expense of deflection.[2-7] In each case some finite amount of total work was lost in the conversion process while weight, volume, complexity and cost penalties were incurred. Because many classes of aircraft have extremely tight weight, volume and performance requirements, they tend to drive actuators to smaller packages with higher levels of performance. Several other classes of piezoelectric actuators to be investigated as of late employ dynamic effects of oscillating piezoelectric, electrostrictive and/or magnetostrictive elements in linear- and rotary-inchworm type motors. Although well suited for some applications, their system-level power densities, bandwidths, form factors and costs are currently not compatible with some of the most demanding classes of aircraft.

Among these most demanding types of aircraft are the small uninhabited aerial vehicles (UAVs), known as mini- or micro-aerial vehicles (MAVs). Similarly, guided hard-launched munitions also present similar challenges to the design engineer with bandwidths ranging in excess of 300 Hz at setback accelerations of upwards of 100,000g's. In recent years, these extreme requirements in bandwidth, weight, volume, environmental and deflection requirements have lead to the development of new, high performance actuators which are specifically tailored to these types of aircraft.[8-10] Figure 1 shows the first MAV which was enabled by piezoelectric Flexspar flight control actuators now more than a decade ago.

Fig. 1 The Lutronix Kolibri, the World's First VTOL MAV Enabled by Piezoelectric Flexspar Stabilators (1997)[11]

Although these actuators have been shown to work for many classes of aircraft, their performance could be improved still further. Although previously unpublished, it is well known by those who work with many of these classes of flight control actuators, that deadband, slop and power density are often challenging issues for the design engineer to work around.

One of the most capable UAVs which has been developed to date is the XQ-138.[11] The XQ-138 is designed to take-off and land vertically, hover like a helicopter, then pitch over and transition to airplane-mode flight for dash out, cruise and loiter to speeds in excess of several hundred kts. Because this class of convertible UAVs is also intended to operate in urban and forested environments in any type of weather, the demands on the flight control assembly are extremely high. Accordingly, PBP/DEAS actuators have been shown to increase useful load and performance with lighter weight, lower power consumption and higher bandwidth than conventional actuators.

Because nearly all actuator schemes which have employed piezoelectric actuators have been centered on various arrangements that trade force for stroke while degrading the total work available, a new approach is needed. In the late'90's Lesieutre conceived a piezoelectric transformer which was designed with axially compressed piezoelectric elements.[12] The axial compression levels were close to the buckling load which effectively nulled some of the loss generating mechanism inherent in most piezoelectric actuator designs. References 12 and 13 showed that by doing this, the overall energy conversion efficiency of the entire system could be made higher than the efficiency of the raw material itself. Accordingly, this paper lays out several years of research which have been centered on improving and bringing this fundamental discovery to the aerospace flight controls community.

Although the technical community has seen successful application of piezoelectric flight control actuators in uninhabited aerial vehicles and micro aerial vehicles, few applications in air-to-ground weapon systems have

surfaced. Because key technologies expanding the capabilities of piezoelectric actuator elements as air-to-ground flight control devices have been methodically matured overseas, patented and subsequently imported to the US, this document will be the first publicly presented work laying out the fundamentals of such advanced actuator elements. This work represents a very high stage of maturity as evidenced by its bench, wind tunnel and flight test record, level of patent protection and current licensing agreements in place and under negotiation. Similarly, it is unfortunate that the conference organizers relegated this work to a silent synopsis, indicating the technical community's lack of understanding of the importance of this branch of technology and its level of maturity.

2. ANALYTICAL MODELING

2.1 Generic Actuator Set-Up

To take advantage of the principles laid out in Ref. 12 and 13, a piezoelectric bender element is arranged in a pin-pin configuration with an externally applied axial force which is close to the perfect column buckling load. The axial force, F_a, is applied so that as the piezoelectric moment is applied, a controlled "imperfection" induces further, but controlled deformation. The overall goal of this Post-Buckled Precompressed (PBP) actuator assembly is to simultaneously and controllably amplify both the force and deflection levels which can be generated by solid state piezoelectric bender elements. The addition of various forms of compliant mechanisms on either end of the actuator allow for a higher level of controllability, but generally retard the ultimate deflection levels so the size, weight and complexity of such mechanisms are typically minimized. Because essentially any level of deflection can be excited via the application of ever higher loads, great care is taken in the design as the external face of the convex actuator element will suffer from various forms of tensile failure including depoling and mechanical fracture if the bending levels are too high. Figure 2 shows the overall arrangement of the actuator including the pin-pin supports, axial force and generic end extensions.

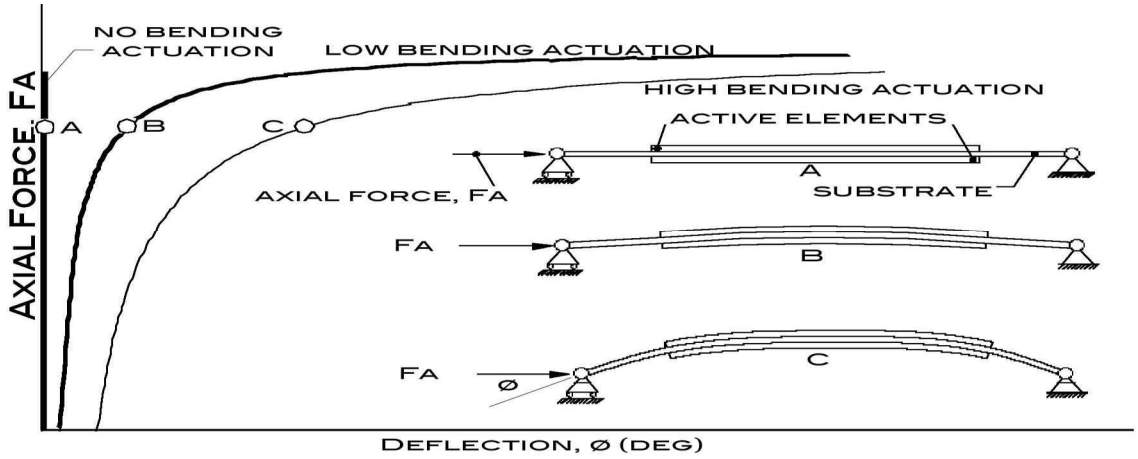

Figure 2 Generic Arrangement of the Post-Buckled Precompressed (PBP) Actuator Arrangement

The static behavior of the unloaded PBP bender element is easily captured by using classical laminated plate theory (CLPT) models. The bender is made from two primary components: a pair of piezoelectric actuator sheets bonded to a structurally stiff substrate. As the piezoelectric sheets are commanded to alternatively expand and contract, the bender element deflects up and down. An important aspect of the design involves the use of coefficient of thermal expansion (CTE) mismatch which has been used for more than 20 years to precompress tension-sensitive piezoceramic elements and pretension usually metallic isotropic substrates.[7,10] The static, unloaded (F_a= 0) behavior of the device can be modeled easily by the techniques described in Ref. 1 and 14. Assuming an unloaded structure and using CLPT methods, the following holds. The applied forces and moments may be balanced by stress distributions which are distributed through the thickness of the element:

$$N = \int \sigma dz \qquad M = \int \sigma Z dz \tag{1}$$

Actuator in-plane forces and moments (a) can be expressed as a balance with external forces and moments (ex) and forces and moments due to mismatches in coefficients of thermal expansion (t). These factors will generate in-plane laminate strains, ε and curvatures, κ.

$$\begin{Bmatrix} N \\ M \end{Bmatrix}_{ex} + \begin{Bmatrix} N \\ M \end{Bmatrix}_{a} + \begin{Bmatrix} N \\ M \end{Bmatrix}_{t} = \begin{bmatrix} A & B \\ B & D \end{bmatrix}_{l} \begin{Bmatrix} \varepsilon \\ \kappa \end{Bmatrix}_{l} \tag{2}$$

If the external forces and moments are ignored and thermally induced stresses are not considered, equation 2 can be reduced to:

$$\begin{bmatrix} A & B \\ B & D \end{bmatrix}_{l} \begin{Bmatrix} \varepsilon \\ \kappa \end{Bmatrix} = \begin{bmatrix} A & B \\ B & D \end{bmatrix}_{a} \begin{Bmatrix} \Lambda \\ 0 \end{Bmatrix} \tag{3}$$

At this point, equation 3 can be easily solved for laminate curvature, κ, by assuming that a balanced, symmetric laminate composed of isotropic or quasi-isotropic elements are used:

$$\kappa = \frac{B_a}{D_l} \Lambda \tag{4}$$

By using the unloaded laminate curvature, κ, as a starting point, the problem can now be defined in terms of gross curvatures with externally applied axial force, F_a, as follows:

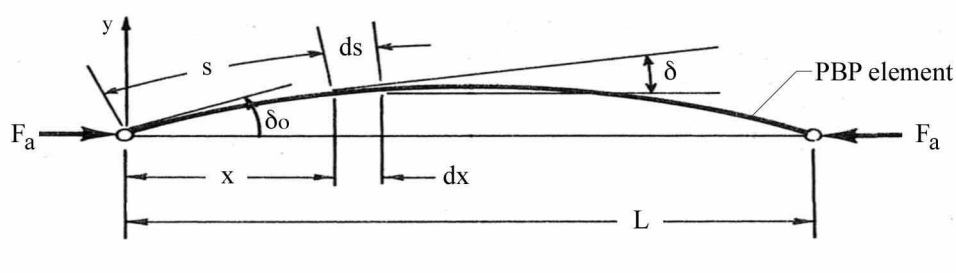

Figure 3 Analysis Terms and Conventions for Analysis of the PBP Actuator Arrangement

Figure 3 shows that the length along the surface of the element, s, and the length along the major axis of the element, x, are related by the curvature induced in the actuator. The angular coordinate, δ is maximized at the ends of the element, δ_o and goes to zero at the mid point.

One can consider the normal strain of any point in the PBP actuator at a distance y from the neutral axis through its thickness as:

$$\varepsilon = \frac{yd\delta}{ds} = \frac{\sigma}{E} \tag{5}$$

If one examines the individual beam element and assumes pure bending, then the following holds:

$$\sigma = \frac{My}{I} \tag{6}$$

Accordingly, combining equations 5 and 6 with CLPT conventions and terminology, equation 7 is obtained:

$$\frac{yd\delta}{ds} = \frac{My}{Db} \tag{7}$$

Because the externally applied moment loading in each section comes from the axial force, F_a:

$$M = -F_a y \tag{8}$$

Substituting equation 8 into 7 yields:

$$\frac{d\delta}{ds} = -\frac{F_a y}{Db} \tag{9}$$

Differentiating equation 9 with respect to s:

$$\frac{d^2\delta}{ds^2} = -\frac{F_a}{Db} Sin\delta \tag{10}$$

Multiplying through by the integrating factor $2 d\delta / ds$:

$$2\frac{d\delta}{ds}\frac{d^2\delta}{ds^2} = -2\frac{F_a}{Db} Sin\delta \frac{d\delta}{ds} \tag{11}$$

Integrating equation 11 yields:

$$\left(\frac{d\delta}{ds}\right)^2 = 2\frac{F_a}{Db} Cos\delta + a \tag{12}$$

If one considers the addition of an applied moment via piezoelectric elements as generating an imperfection across the beam, then the unknown integrating factor, a, can be solved for, given that at x=0, $\delta = \delta_o$, $d\delta / ds = \kappa$.

$$\left(\frac{d\delta}{ds}\right)^2 = 2\frac{F_a}{Db}\left(Cos\delta - Cos\delta_o\right) + \kappa^2 \tag{13}$$

With appropriate trigonometric substitutions and considering the negative root because dδ is always negative:

$$\frac{d\delta}{ds} = -2\sqrt{\frac{F_a}{Db}}\sqrt{Sin^2\left(\delta_o/2\right) - Sin^2\left(\delta/2\right) + \frac{\kappa^2 Db}{4F_a}} \tag{14}$$

For solution, a change of variable is as follows:

$$Sin\left(\delta/2\right) = c Sin\xi \tag{15}$$

Where ξ is a variable with the value π/2 when x = 0 and the value 0 when x = L/2. Accordingly, when x = 0:

$$c = Sin\left(\delta_o/2\right) \tag{16}$$

Solving for δ and differentiating yields:

$$\delta = 2Sin^{-1}\left(Sin\left(\delta_o/2\right)Sin\xi\right) \qquad d\delta = \frac{2Sin\left(\delta_o/2\right)Cos\xi}{\sqrt{1 - Sin^2\left(\delta_o/2\right)Sin^2\xi}}d\xi \tag{17}$$

Combining equations 14 through 17 with appropriate end values:

$$\sqrt{\frac{F_a}{Db}}\int_0^{L/2} ds = \frac{L}{2}\sqrt{\frac{F_a}{Db}} = \int_0^{\pi/2} \frac{Sin\left(\delta_o/2\right)Cos\xi}{\left(\sqrt{Sin^2\left(\delta_o/2\right)Cos^2\xi + \frac{\kappa^2 Db}{4F_a}}\right)\left(\sqrt{1 - Sin^2\left(\delta_o/2\right)Sin^2\xi}\right)}d\xi \tag{18}$$

3. ACTUATOR DESIGN AND FABRICATION

3.1 Overall Design

Reference 15 lays out the fundamental operating characteristics and design of Post-Buckled Precompressed (PBP) actuators along with Dynamic Elastic Axis Shifting (DEAS) structures. Figure 4 shows the basic structure of a PBP/DEAS actuator element with both externally applied forces (50) and precompression straps (20). The adaptive material core (10-40) provides an initial bending imperfection so as to initiate bending.

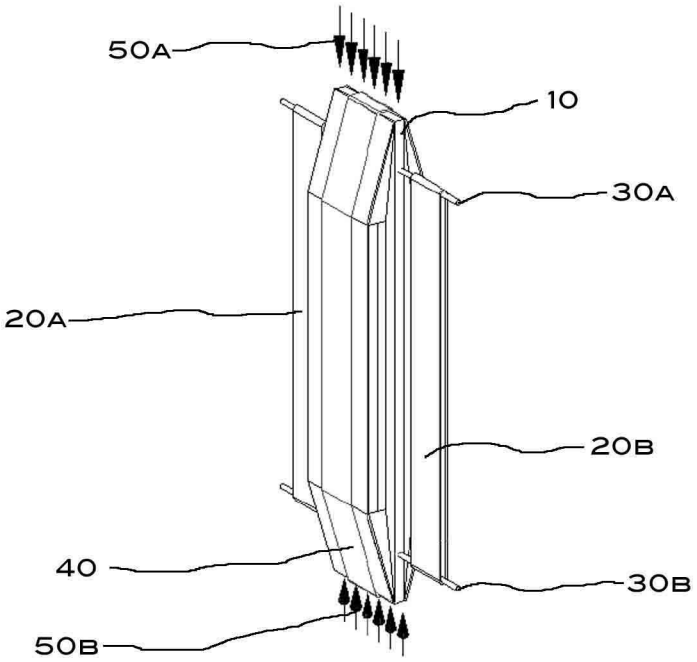

Fig. 4 Post-Buckled Precompressed (PBP)/Dynamic Elastic Axis Shifting (DEAS) Actuator Element[15]

If one examines the individual components of the PBP/DEAS actuator, the role of each part becomes more clear as seen in Fig. 5. Joining the active elements to the substrate are both structural and electrically conductive materials (130). The substrate (10) typically supports some mechanics which can impart an axially precompressive load such as the loading posts (30). These transmit axial forces to the actuator. There is also an external strap (40) which can come off the concave face of the actuator during deflections. One of the most important features of the PBP/DEAS actuator is the facing sheets (110). These facing sheets act to place the convex actuator elements in compression during high deflection actuation. Because these elements normally either catastrophically fail in tension or depole due to excessive in-plane stresses, the functionality of the facing sheets is imperative. Their effectiveness is aided by spacers (100) and end resin plugs (80). Both of which help transmit shear forces to the substrate.

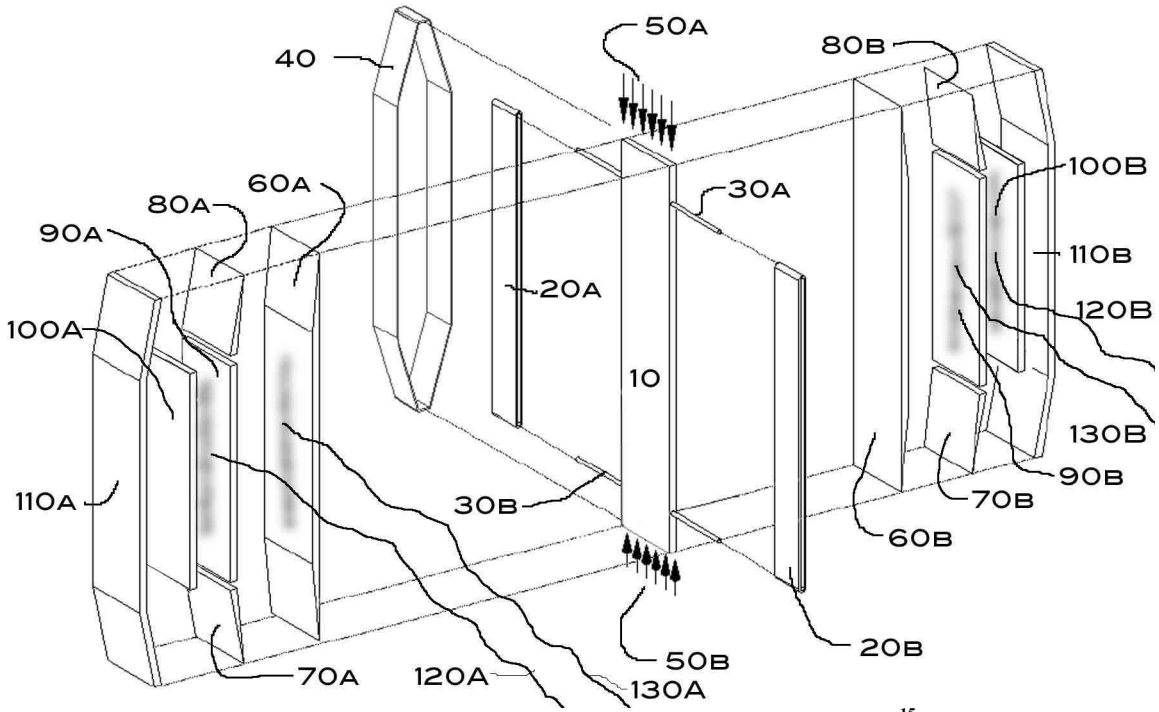

Fig. 5 Exploded View of the PBP/DEAS Actuator Element[15]

Reference 15 includes many incarnations of the PBP/DEAS Actuator Assembly including body mounted missile and munition configurations.

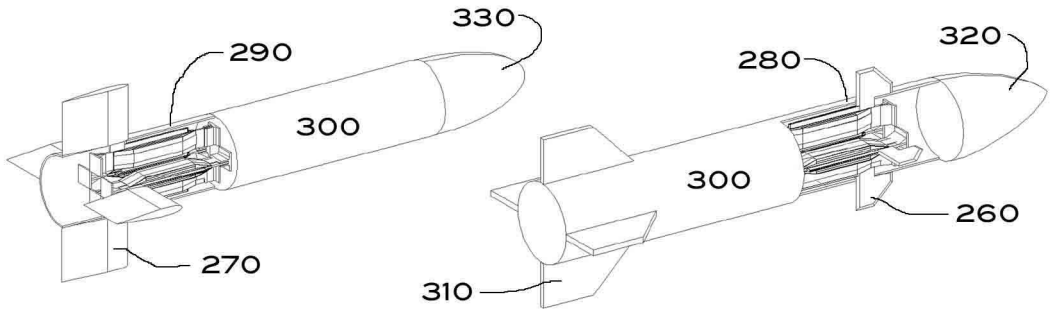

Fig. 6 Two Sample PBP/DEAS Actuator Integration Schemes from Ref. 15

One of the more advanced concepts of actuation is completely contained within a given flight control surface or fin. If one designs an aerodynamic flight control surface for a typical gravity weapon, it should take a transonic profile given contemporary drop conditions. With a transonic flight profile, the aerodynamic center location varies from the quarter-chord to the half chord of the surface. A simple routine can be run to establish a minimum moment location over typical deflections. Considering a low aspect ratio rounded diamond profile aerodynamic profile, the main spar should be placed close to the 1/3 chord for aerodynamic moment minimization. Figure 7 shows the PBP/DEAS fin with main spar properly placed. Because all of the actuator elements are contained within the fin itself, it can be placed adjacent to warheads without penetrating hardened steel casings. Also important is the placement of the canard set as to enable translate-to-turn end-game maneuver capability rather than skid-to-turn maneuvers which induces high impact angularity, increasing skip probability. References 16 through 19 show several other applications and incarnations of PBP/DEAS actuators in aerospace systems.

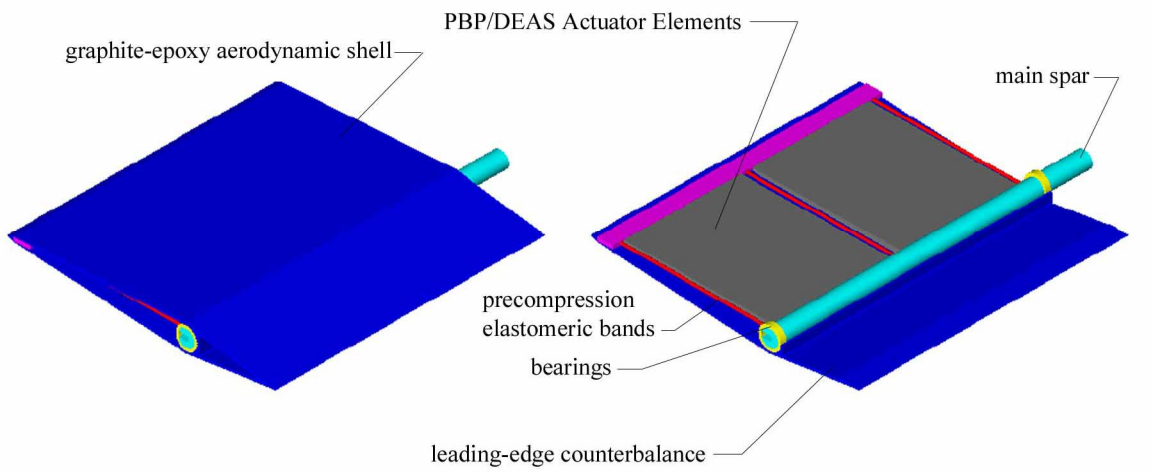

Fig. 7 6" (15.2cm) Square Rounded Diamond, Transonic Profile PBP/DEAS Flight Control Surface Layout

3.2 PBP/DEAS Flight Control Surface Fabrication

The PBP/DEAS flight control surface was sized for a typical 250lb (113kg) small gravity weapon. Figure 8 shows the actuator core with main spar, bearings, precompression elastic bands and graphite-epoxy aerodynamic shell. Designed to accept airloads through Mach 1.3 with a structural safety factor of 3 and fold capability, the PBP/DEAS surface is ideally suited for flight control over conventional electromechanical actuators.

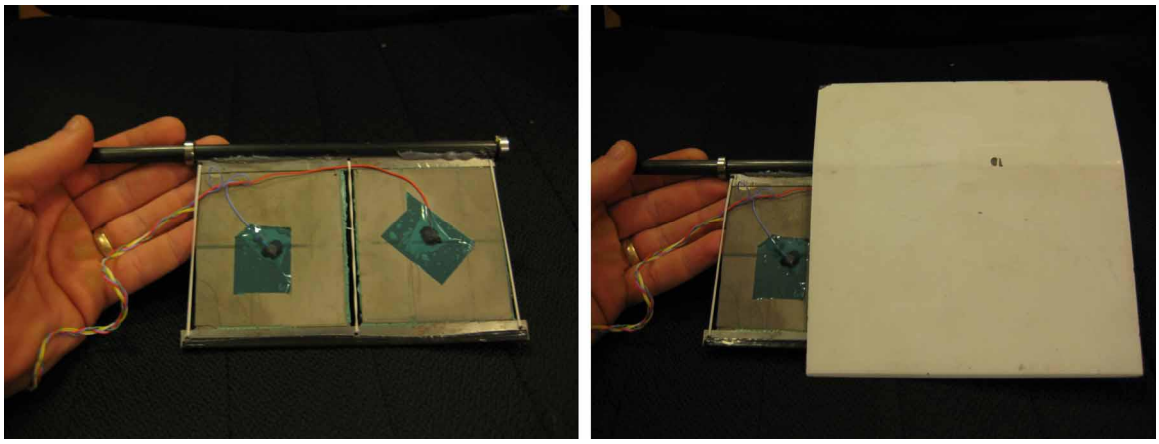

Fig. 8 PBP/DEAS Experimental Test Article Actuator Core and Assembly into Aeroshell

4. EXPERIMENTAL TESTING AND RESULTS

4.1 Quasi-Static Bench Testing

A series of bench tests were conducted to verify quasi-static and dynamic deflection characteristics with varying input signals. Figure 9 shows the amount of rotational deflection as a function of axial pretention on the elastomeric bands. Fig. 9 shows the amount of precompression in terms of gmf per unit of span. Testing was conducted with a 1 Hz sinusoidal signal driving the fin open loop. From Fig. 9, it can be seen that the deflections increase dramatically with both level of axial force and voltage which induces greater and greater levels of imperfection. It should be noted that the fin maintains excellent blocked force resistance capability even at higher rotational deflections. This is because the PBP effect effectively expands the total force-deflection envelope of the entire actuator assembly. The bump stop boundary seen at the right of the figure at 7° is critical as it represents the deflection level associated with onset of mechanical failure of the elements. Beyond 7° facing

sheets kick in and further precompress the actuator core, thereby saving the actuator assembly from depoling and/or mechanical failure.

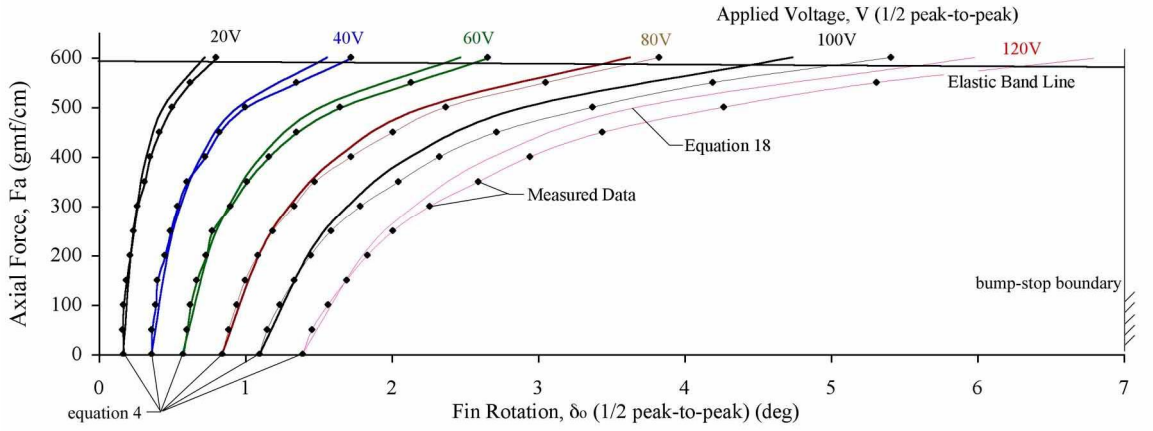

Fig. 9 Correlation of PBP/DEAS Fin Deflection and Theory

4.2 Wind Tunnel Testing

A series of wind tunnel tests were conducted to ensure that no flutter or divergence tendencies were present and that deflections remain steady with airspeed. Wind tunnel testing was conducted in the University of Kansas 3' x 4' (91cm x 122cm) subsonic wind tunnel at speeds up to 120 ft/s (71kts, 82mph, 36.5m/s). Figure 10 shows that the deflections are neither amplified nor degraded with increased airflow up through the test speeds. Because the aerodynamic center, center of gravity and center of pressure are all close to the hinge line of the fin, coupling pitch deflections and flutter tendencies are effectively nulled as seen in Fig. 10.

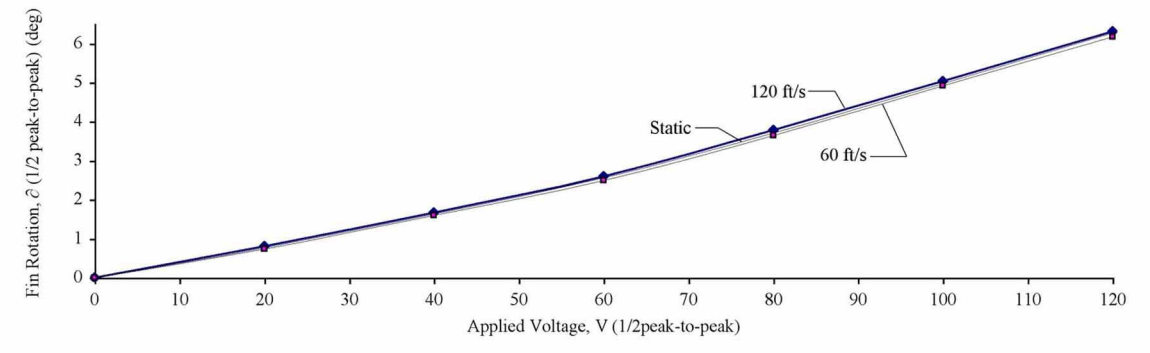

Fig. 10 PBP/DEAS Fin Performance in Wind Tunnel up to 120 ft/s (71kts, 36.5m/s)

To fully appreciate the utility of the PBP/DEAS actuator assembly, a side-by-side comparison of the PBP/DEAS actuator fin and a conventional electromechanical servomechanism similar to those used in conventional gravity weapons described above is laid out:

Table 1 Comparison of PBP and Conventional Electromechanical Pitch and Yaw Flight Control Actuator Systems

	Conventional Servoactuaor	PBP Actuator
max power	24W	1.3W
max current	5A	18mA
mass	108 g	73g
slop	1.6°	0.02°
break frequency	3Hz	21 Hz
part count	56	6

CONCLUSIONS

It has been shown that a new class of adaptive transonic gravity weapon flight control mechanisms using Post-Buckled Precompressed (PBP) Dynamic Elastic Axis Shifting (DEAS) actuators works well. Providing deflection levels in excess of ±7° at rates through 21 Hz and Mach 1.3, for less than 1.3W of peak power, the 6" (15.2cm) rectangular transonic fin is ideally suited for many gravity weapon configurations. Additionally, because of the low profile of the actuator assembly, it can be packed completely within the aeroshell thereby negating the need for occupation of additional volume within wareheads or fuselages. It has been shown that theoretical estimations of pitch deflections using laminated plate theory, kinematics and imperfection level determination adequately captures the performance of the PBP/DEAS fin.

ACKNOWLEDGMENTS

The authors would like to acknowledge the outstanding contributions of the many students and colleagues who helped with this study including Dr. Paolo Tiso of TU Delft Faculty of Aerospace Engineering and Mr. Wes Ellison of The University of Kansas Aerospace Engineering Department.

REFERENCES

1. Crawley, E. F. and De Luis, Javier, "Use of Piezoelectric Actuators as Elements of Intelligent Structures," *AIAA Journal,* Vol. 25, No. 10, Oct. 1987, pp. 987-997.
2. Prechtl, E.F. and Hall, S. R., "Design of a High Efficiency, Large Stroke Electromechanical Actuator," Journal of Smart Materials and Structures, published by IOP Publishing, Bristol, UK, Vol. 8, pp. 13 – 30, 1999.
3. J. Moskalik and D. Brei, 1998, "Analytical Dynamic Performance Modeling for Individual C-Block Actuators," *Journal of Vibrations and Acoustics*, Vol. 121, pp. 221-230.
4. A.J. Moskalik and D. Brei, 1999, "Force-Deflection Behavior of Piezoelectric C-Block Actuator Arrays," *Smart Materials and Structures*, Vol. 8, pp.531-543.
5. J. Ervin and D. Brei, December 1998, "Recurve Piezoelectric-Strain-Amplifying Actuator Architecture", *IEEE/ASME Transactions on Mechatronics*, Vol. 3, No. 4, pp. 293-301.
6. Clement, J., Brei, D., Moskalik, A., and Barrett, R., "Bench-Top Performance Characterization of a C-Block Driven Active Flap System," proceedings of the 39th Structures, Structural Dynamics and Materials Conference 20 - 23 April 1998, Long Beach, CA, published by the American Institute of Aeronautics and Astronautics, Washington, D.C. 1998, paper no. AIAA-98-2039.
7. Schwartz, R. W., Laoratanakul, P., Nothwang, W. D., Ballato, J., Moon, Y. and Jackson, A., "Understanding Mechanics and Stress Effects in Rainbow and Thunder Actuators," *SPIE Smart Structures and Materials, Active materials: Behavior and Mechanics*, 3992, 363 (2000).
8. Barrett, R., Burger, C., and Melian, J. P., "Recent Advances in Uninhabited Aerial Vehicle (UAV) Flight Control with Adaptive Aerostructures," Proceedings of the 4th European Demonstrators Conference, 10 – 15 December 2001, Edinburgh, Scotland.
9. Barrett, R. and Lee, G., "Design Criteria, Aircraft Design, Fabrication and Testing of Sub-Canopy and Urban Micro-Aerial Vehicles," proceedings of the AIAA/AHS International Powered Lift Conference, Alexandria, Virginia, 1 November 2000.
10. Barrett, R., and Stutts, J., "Development of a Piezoceramic Flight Control Surface Actuator for Highly Compressed Munitions," proceedings of the 39th Structures, Structural Dynamics and Materials Conference 20 - 23 April 1998, Long Beach, CA, published by the American Institute of Aeronautics and Astronautics, Washington, D.C. 1998, paper no. AIAA-98-2034.
11. Barrett, R., "Adaptive Aerostructures, Improving High Performance, Subcale Military UAVs," 45th AIAA/ASME/ASCE/AHS/ASC Structures, Structural Dynamics and Materials Conference, 12th

AIAA/ASME/AHS Adaptive Structures Conference 19 – 22 April 2004/Palm Springs, California, AIAA paper no. 2004-1886.

12. Lesieutre, G.A., and C.L. Davis, “Can a Coupling Coefficient of a Piezoelectric Actuator be Higher Than Those of Its Active Material?,” Journal of Intelligent Materials Systems and Structures, Vol. 8, 1997, pp. 859-867.
13. Lesieutre, G. A. and Davis, C. L., “Transfer Having a Coupling Coefficient Higher than its Active Material,” US Pat. 6,236,143 issued 22 May 2001.
14. Jones, R. M., "Micromechanical Behavior of a Lamina," *Mechanics of Composite Materials*, Hemisphere Publishing Corporation, New York, 1975
15. Barrett, R. and P. Tiso, “PBP Adaptive Actuator Device and Embodiments,” International Patent Application number PCT/NL2005/000054, via TU Delft, 18 February 2005.
16. Barrett, R., Vos, R., Tiso, P. and De Breuker, R., "Post-Buckled Precompressed (PBP) Actuators: Enhancing VTOL Autonomous High Speed MAVs," Proceedings of the 46th AIAA/ASME/ASCE/AHS/ASC Structures, Structural Dynamics and Materials Conference , Austin, Texas, Apr. 18-21, 2005, AIAA paper no. AIAA-2005-2113.
17. Vos, R., De Breuker, R., Barrett, R. and Tiso, P., " Morphing Wing Flight Control Via Post-Buckled Precompressed Piezoelectric Actuators," AIAA Journal of Aircraft, Vol. 44, No. 4 0021-8669, 2007.
18. Barrett, R., McMurtry, R., Vos, R.., Tiso, P. and De Breuker, R., "Post-Buckled Precompressed Piezoelectric Flight Control Actuator Design, Development and Demonstration," Journal of Smart Materials and Structures, Volume 15, No. 5, October 2006 1323 - 1331.
19. De Breuker, R., Vos, R., Barrett, R. and Tiso, P., "Nonlinear Semi-Analytical Modeling of Post-Buckled Precompressed (PBP) Piezoelectric Actuators for UAV Flight Control," Proceedings of the 47th AIAA/ASME/ASCE/AHS/ASC Structures, Structural Dynamics, and Materials Conference 14th AIAA/ASME/AHS Adaptive Structures Conference 7th, Newport, Rhode Island, May 1-4, 2006 AIAA-2006-1795.

View publication stats